

Photodiode characteristics and band alignment parameters of epitaxial $\text{Al}_{0.5}\text{Ga}_{0.5}\text{P}$

An Chen^{1,a)} and Jerry M. Woodall²

¹Department of Electrical Engineering, Yale University, New Haven, Connecticut 06511, USA

²School of Electrical and Computer Engineering, Purdue University, West Lafayette, Indiana 47907, USA

(Received 29 November 2008; accepted 17 December 2008; published online 12 January 2009)

Wide-bandgap semiconductor $\text{Al}_x\text{Ga}_{1-x}\text{P}$ is a promising material candidate for low-noise photodiodes in blue/UV spectrum. Photodiodes were fabricated on $\text{Al}_{0.5}\text{Ga}_{0.5}\text{P}$ epitaxial layer grown lattice matched on GaP substrate by molecular beam epitaxy. Although quantum efficiency is low for standard p - i - n photodiode due to inadvertent photon absorption in the top p -layer, it can be significantly improved by opening a recessed window in the top p -layer or by using a Schottky junction photodiode structure. $\text{Al}_{0.5}\text{Ga}_{0.5}\text{P}$ band alignment parameters can be extrapolated from the current-voltage characteristics of $\text{Al}_{0.5}\text{Ga}_{0.5}\text{P}$ Schottky junctions. The bandgap of $\text{Al}_{0.5}\text{Ga}_{0.5}\text{P}$ was measured to be 2.38 eV. © 2009 American Institute of Physics. [DOI: 10.1063/1.3069282]

Ternary compound semiconductor $\text{Al}_x\text{Ga}_{1-x}\text{P}$ offers promising properties for optoelectronic device applications.^{1,2} The addition of Al to GaP enlarges the bandgap of the ternary compound³ and shifts its photoemission peaks to shorter wavelengths, enabling it for green-light emission devices.⁴⁻⁶ With low intrinsic carrier concentration, $\text{Al}_x\text{Ga}_{1-x}\text{P}$ can be utilized in low-noise and high-temperature applications.⁷ Similar to the $\text{Al}_x\text{Ga}_{1-x}\text{As}$ -GaAs material system, $\text{Al}_x\text{Ga}_{1-x}\text{P}$ and GaP are closely lattice matched for all Al composition,⁸ providing a suitable heterostructure for optical waveguides⁹ and quantum well devices.¹⁰ $\text{Al}_x\text{Ga}_{1-x}\text{P}$ can also be used as a transparent window on GaP devices. These interesting characteristics notwithstanding, experimental research related to $\text{Al}_x\text{Ga}_{1-x}\text{P}$ has been very limited, partially due to the concern regarding the material stability of $\text{Al}_x\text{Ga}_{1-x}\text{P}$. It is expected that $\text{Al}_x\text{Ga}_{1-x}\text{P}$ with high Al concentration may decompose in atmosphere due to oxidation reactions.¹¹ Lack of experimental data has also limited the knowledge of band alignment properties of $\text{Al}_x\text{Ga}_{1-x}\text{P}$ /GaP heterojunction, but some parameters have been obtained from theoretical estimation¹²⁻¹⁴ and experimental investigation.^{15,16} It is generally believed that $\text{Al}_x\text{Ga}_{1-x}\text{P}$ /GaP is a type-II heterojunction (i.e., staggered gaps) with both E_C and E_V of GaP shifted upward from the E_C and E_V of $\text{Al}_x\text{Ga}_{1-x}\text{P}$.¹²

In recent experiments, we have grown $\text{Al}_x\text{Ga}_{1-x}\text{P}$ epilayers on GaP substrate by molecular beam epitaxy (MBE) with Al composition up to 75%. Our results have shown that epilayers with these compositions were stable in atmosphere for extended period of time. In addition, the $\text{Al}_x\text{Ga}_{1-x}\text{P}$ epilayers in our experiments were protected by GaP cap layers, which also helped to improve their stability. $\text{Al}_{0.5}\text{Ga}_{0.5}\text{P}$ -based photodiodes with various structures were fabricated and characterized. Their spectrum response was measured in the wavelength range from 650 to 400 nm. This paper reports the characteristics of these photodiodes on epitaxial $\text{Al}_{0.5}\text{Ga}_{0.5}\text{P}$.

Figure 1 shows the structure of the MBE sample for photodiodes. A 2 μm thick undoped i - $\text{Al}_{0.5}\text{Ga}_{0.5}\text{P}$ was grown between a p^+ layer (doped to 10^{20} cm^{-3} with Be) and

a n^+ layer (doped to $5 \times 10^{18} \text{ cm}^{-3}$ with Si), which forms a p - i - n structure for photodiodes. The p^+ layer above i - $\text{Al}_{0.5}\text{Ga}_{0.5}\text{P}$ was graded from $\text{Al}_{0.5}\text{Ga}_{0.5}\text{P}$ to GaP in composition through a 0.04 μm thick layer, followed by a 0.05 μm thick p^+ GaP cap layer. The n^+ layer below i - $\text{Al}_{0.5}\text{Ga}_{0.5}\text{P}$ was also graded from $\text{Al}_{0.5}\text{Ga}_{0.5}\text{P}$ to GaP. The composition-grading layers were grown to minimize the effects of an abrupt $\text{Al}_x\text{Ga}_{1-x}\text{P}$ /GaP interface and the band offset on carrier transport. The p - i - n structure was grown on n -type GaP substrate, with a 0.5 μm thick GaP layer and a 0.1 μm thick $\text{Al}_{0.5}\text{Ga}_{0.5}\text{P}$ layer as buffer layers in between. The buffer layers help to minimize the impurity diffusion from the substrate into the active device layers. The p - i - n structure is preferred to p - n junction for photodiode applications because the i -layer width can be designed to optimize the quantum efficiency (QE). Wider i -layer allows more photons to be absorbed and improves efficiency; however, there exists a trade-off between efficiency and speed.

To fabricate photodiodes, a mesa was etched through the p - i - n structure into the n^+ -layers to define the diode size using $\text{HCl}(36\%):\text{HNO}_3(65%):\text{H}_2\text{O}$ (1:1:1 in volume ratio).

0.05 μm GaP, p^+ 10^{20} cm^{-3} Be-doped
0.04 μm $\text{Al}_{0.5}\text{Ga}_{0.5}\text{P}$ graded to GaP, p^+ 10^{20} cm^{-3} Be-doped
2.0 μm $\text{Al}_{0.5}\text{Ga}_{0.5}\text{P}$, undoped
0.04 μm GaP graded to $\text{Al}_{0.5}\text{Ga}_{0.5}\text{P}$, n^+ $5 \times 10^{18} \text{ cm}^{-3}$ Si-doped
0.05 μm GaP, n^+ $5 \times 10^{18} \text{ cm}^{-3}$ Si-doped
0.1 μm $\text{Al}_{0.5}\text{Ga}_{0.5}\text{P}$, n^+ $5 \times 10^{18} \text{ cm}^{-3}$ Si-doped
0.5 μm GaP, n^+ $5 \times 10^{18} \text{ cm}^{-3}$ Si-doped
n -type GaP substrate

FIG. 1. The structure of $\text{Al}_{0.5}\text{Ga}_{0.5}\text{P}$ p - i - n MBE sample grown on GaP substrate for the fabrication of photodiodes.

^{a)}Electronic mail: an.chen@aya.yale.edu.

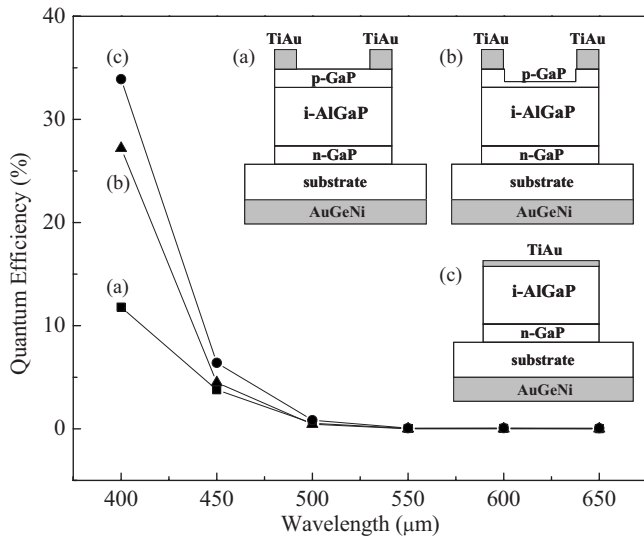


FIG. 2. The measured external QE of $\text{Al}_{0.5}\text{Ga}_{0.5}\text{P}$ photodiodes in the wavelength range from 400 to 650 nm for three different photodiode structures. The insets show the three different structures. Diode (a) has $p\text{-GaP}/i\text{-Al}_{0.5}\text{Ga}_{0.5}\text{P}/n\text{-GaP}$ structure with ring-shaped metal contact on top. Diode (b) has $p\text{-GaP}/i\text{-Al}_{0.5}\text{Ga}_{0.5}\text{P}/n\text{-GaP}$ structure with a recess window etched in the top $p\text{-GaP}$ layer. Diode (c) has metal/ $i\text{-Al}_{0.5}\text{Ga}_{0.5}\text{P}/n\text{-GaP}$ Schottky junction structure with very thin (~ 10 nm) metal contact. The insets ignored the composition-grading layers at p - i and i - n interfaces.

Ohmic contact for the n -layer was made with alloyed Au-Ge-Ni on the back side of the GaP substrate. Front metal contact was made with nonalloyed TiAu on heavily doped p^+ -GaP layer.¹⁷ Three different photodiode structures were fabricated and characterized, as shown in Fig. 2. Structure (a) is a standard p - i - n photodiode, where a ring-shaped metal contact (TiAu) was deposited by e-beam evaporator on the top p^+ -GaP layer for device probing. Although this structure is simple for fabrication, its QE is degraded by absorption of photons and recombination of the generated electron-hole (e-h) pairs in the top p -layers. This QE loss is especially severe in short wavelength spectrum where the photon penetration depth is shallow and a large portion of photons is absorbed in the top GaP layer instead of in the active $\text{Al}_{0.5}\text{Ga}_{0.5}\text{P}$ layer below. To reduce the QE loss, structure (b) employs a recessed window by etching part of the top p -layers in the center of the ring contact. Structure (c) is a Schottky junction photodiode, where the top p -layers were removed by etching. A very thin (~ 10 nm) metal layer was deposited directly on top of undoped $\text{Al}_{0.5}\text{Ga}_{0.5}\text{P}$ to form a metal-semiconductor junction.

Figure 2 shows the external QE of the three photodiode structures in the wavelength range of 650–400 nm. The measurement equipment limited the shortest wavelength to 400 nm. The photodiodes were reverse biased at -10 V. Because the undoped i -layer is fully depleted, the measured QE only varies slightly with reverse bias voltage. The long-wavelength cutoff for all devices is between 500 and 550 nm, corresponding to a bandgap in the range of 2.25–2.48 eV. It will be shown later that the bandgap of the epitaxial $\text{Al}_{0.5}\text{Ga}_{0.5}\text{P}$ was measured to be ~ 2.38 eV. QE increases quickly with decreasing wavelength due to higher absorption coefficient at shorter wavelength. With further decrease in wavelength, QE may start to decrease due to increasing surface absorption/recombination and result in a peak in the spectral response, which was not observed in this

measurement due to limited wavelength range. The QE of the standard p - i - n photodiode, i.e., structure (a), is quite low because of photon absorption in the top p -layers. The absorption coefficient of GaP at photon energy of 3.1 eV (i.e., $\lambda = 400$ nm) is $\alpha = 8.63 \times 10^4 \text{ cm}^{-1}$,¹⁸ corresponding to photon penetration depth of $d = 1/\alpha = 116$ nm in GaP. Therefore, more than half of the incident photons were absorbed in the top 50 nm thick p^+ -GaP layer and 40 nm thick composition-grading p^+ -layer, where recombination rate is high due to extremely heavy doping and surface states. Consequently, most e-h pairs generated by these photons recombine without contributing to electrical response. QE can be significantly improved by etching a recessed window in the top p -layers to reduce photon absorption there, as shown by structure (b). The QE of structure (b) is more than twice higher than that of structure (a). Further improvement of QE was achieved in Schottky junction photodiode (c). In structure (c), high electric field exists in the $\text{Al}_{0.5}\text{Ga}_{0.5}\text{P}$ layer underneath the metal-semiconductor junction. The field separates the e-h pairs generated by photons passing through the metal contact, which reduces the probability of recombination and improves QE. By making the metal contact sufficiently thin, the photon absorption in the metal layer can be minimized.

The external QE of Schottky junction photodiode on epitaxial $\text{Al}_{0.5}\text{Ga}_{0.5}\text{P}$ reaches $\sim 34\%$. A ring-shaped thin metal contact was also made for Schottky junction photodiode to increase photon absorption, and the QE was measured to be $>45\%$. However, the electrical field in the i -layer is not in the vertical direction due to the ring-shaped top contact, which may affect the carrier transport and the photodiode response speed. In comparison with GaP-based photodiode,¹⁹ the spectral response of $\text{Al}_{0.5}\text{Ga}_{0.5}\text{P}$ photodiode is shifted to shorter wavelength due to wider bandgap of $\text{Al}_{0.5}\text{Ga}_{0.5}\text{P}$. Further improvement on the efficiency of $\text{Al}_x\text{Ga}_{1-x}\text{P}$ photodiodes may be achieved by reducing surface reflection to maximize photon absorption, by improving the quality of the epitaxial material to reduce recombination, or by optimizing the photodiode structure, etc. Photodiodes based on $\text{Al}_{0.75}\text{Ga}_{0.25}\text{P}$ were also fabricated and characterized. They demonstrated spectral response very similar to that of $\text{Al}_{0.5}\text{Ga}_{0.5}\text{P}$ photodiodes, with slightly higher efficiency. The bandgap difference between $\text{Al}_{0.75}\text{Ga}_{0.25}\text{P}$ and $\text{Al}_{0.5}\text{Ga}_{0.5}\text{P}$ is expected to be ~ 0.05 eV,⁴ corresponding to the long-wavelength cutoff difference of ~ 10 nm, which is too small to be observed in this measurement.

The long-wavelength cutoff in the spectral response in Fig. 2 provides a rough range for the bandgap of $\text{Al}_{0.5}\text{Ga}_{0.5}\text{P}$. This bandgap can be more accurately determined by measuring the barrier heights of Schottky junctions on n - and p -type substrates, Φ_N and Φ_P , respectively. The bandgap can be calculated from $E_G = \Phi_N + \Phi_P$.²⁰ In this experiment, two MBE samples were prepared, with $0.1 \mu\text{m}$ thick undoped $\text{Al}_{0.5}\text{Ga}_{0.5}\text{P}$ layers grown on n^+ and p^+ substrates. Au contact was deposited by e-beam evaporator on these samples to form m - i - n and m - i - p Schottky junctions. Devices were isolated by etching through the $\text{Al}_{0.5}\text{Ga}_{0.5}\text{P}$ layers into the substrates. The current-voltage (I - V) characteristics of these junctions were measured using semiconductor parameter analyzer HP 4156. Figure 3 shows the forward bias I - V characteristics of Schottky junctions on n - and p -type substrates, both demonstrating linear behavior over more than four orders of magnitude on semilogarithm scale. The ideality fac-

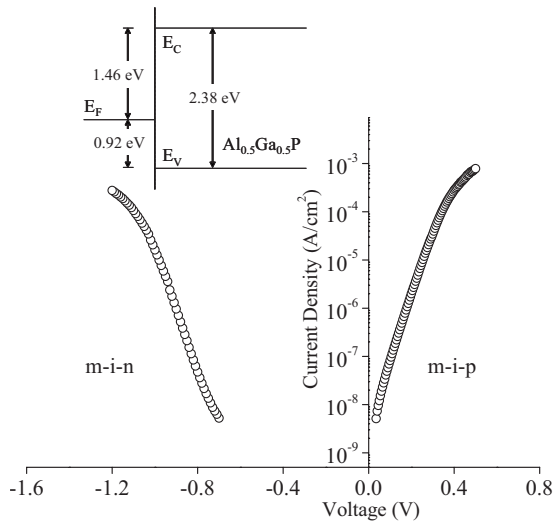


FIG. 3. The forward bias I - V characteristics of Au/ $\text{Al}_{0.5}\text{Ga}_{0.5}\text{P}$ Schottky diodes made on n -type (left panel) and p -type (right panel) substrates. From the I - V curves, the Schottky barrier heights were calculated to be 1.46 and 0.92 eV for junctions on n - and p -type substrates, respectively. The inset shows the Au/ $\text{Al}_{0.5}\text{Ga}_{0.5}\text{P}$ band edge alignment diagram calculated from the I - V characteristics.

tors are calculated to be ~ 1.3 for both junctions. By fitting the I - V characteristics to the thermionic emission-diffusion theory,²⁰ the Schottky junction barrier heights were estimated to be $\Phi_N = 1.46$ eV and $\Phi_p = 0.92$ eV, respectively. Therefore, the bandgap of $\text{Al}_{0.5}\text{Ga}_{0.5}\text{P}$ was calculated to be 2.38 eV. The result matches well with the reported bandgap of 2.37 eV in literature.⁴ It corresponds to a cutoff wavelength of 520 nm in spectral response, consistent with the results in Fig. 2. The band edge alignment diagram for Au/ $\text{Al}_{0.5}\text{Ga}_{0.5}\text{P}$ Schottky junction is shown in the inset in Fig. 3.

Using the Au/ $\text{Al}_{0.5}\text{Ga}_{0.5}\text{P}$ band edge alignment parameters, it is possible to estimate the electron affinity of $\text{Al}_{0.5}\text{Ga}_{0.5}\text{P}$ and to further determine $\text{Al}_{0.5}\text{Ga}_{0.5}\text{P}/\text{GaP}$ band offsets. However, the reliability of the estimation depends on the accuracy of the metal work function. Compared to the Au/ $\text{Al}_x\text{Ga}_{1-x}\text{P}$ band edge alignment parameters in Ref. 12,

our results were larger by 0.08–0.10 eV, which is within the 0.10 eV error margin in this reference. Although it is difficult to accurately estimate $\text{Al}_{0.5}\text{Ga}_{0.5}\text{P}/\text{GaP}$ band offsets here, it is likely that $\text{Al}_{0.5}\text{Ga}_{0.5}\text{P}/\text{GaP}$ is a type-II heterojunction with staggered gaps as suggested in Ref. 12.

In summary, photodiodes were fabricated on $\text{Al}_x\text{Ga}_{1-x}\text{P}$ and the measured QE is promising for photodetector applications in blue/UV spectrum. QE can be significantly improved by optimizing the photodiode structures to reduce inadvertent surface photon absorption and carrier recombination. The bandgap of $\text{Al}_{0.5}\text{Ga}_{0.5}\text{P}$ was measured to be 2.38 eV, based on the I - V characteristics of Schottky junctions. The measured Au/ $\text{Al}_{0.5}\text{Ga}_{0.5}\text{P}$ band edge alignment parameters are consistent with reported results in literature.

¹S. G. Choi, Y. D. Kim, S. D. Yoo, D. E. Aspnes, D. H. Woo, and S. H. Kim, *J. Appl. Phys.* **87**, 1287 (2000).

²J. L. Merz and R. T. Lynch, *J. Appl. Phys.* **39**, 1988 (1968).

³H. Kressel and I. Ladany, *J. Appl. Phys.* **39**, 5339 (1968).

⁴H. Sonomura, T. Nanmori, and T. Miyauchi, *Appl. Phys. Lett.* **24**, 77 (1974).

⁵O. N. Ermakov, R. S. Ignatkina, A. P. Karatsyuba, V. P. Sushkov, and V. F. Aksenov, *IEEE Trans. Electron Devices* **30**, 268 (1983).

⁶H. Sonomura, T. Nanmori, and T. Miyauchi, *Appl. Phys. Lett.* **22**, 532 (1973).

⁷T. E. Zipperian and L. R. Dawson, *J. Appl. Phys.* **54**, 6019 (1983).

⁸A. G. Milnes and D. L. Feucht, *Heterojunctions and Metal-Semiconductor Junctions* (Academic, New York, 1972).

⁹H. P. Kleinknecht and A. E. Widmer, *J. Appl. Phys.* **45**, 3453 (1974).

¹⁰S. Nagao, T. Fujimori, H. Gotoh, H. Fukushima, T. Takano, H. Ito, S. Koshihara, and F. Minami, *J. Appl. Phys.* **81**, 1417 (1997).

¹¹H. Sonomura and T. Miyauchi, *Jpn. J. Appl. Phys.* **8**, 1263 (1969).

¹²S. Tiwari and D. J. Frank, *Appl. Phys. Lett.* **60**, 630 (1992).

¹³S. J. Chua, X. H. Zhang, S. J. Xu, and X. Gu, *J. Phys.: Condens. Matter* **9**, L279 (1997).

¹⁴S. H. Wei and A. Zunger, *Appl. Phys. Lett.* **72**, 2011 (1998).

¹⁵J. R. Waldrop, R. W. Grant, and E. A. Kraut, *J. Vac. Sci. Technol. B* **11**, 1617 (1993).

¹⁶A. Morii, H. Okagawa, K. Hara, J. Yoshino, and H. Kukimoto, *Jpn. J. Appl. Phys., Part 2* **31**, L1161 (1992).

¹⁷M. V. Tagare, T. P. Chin, and J. M. Woodall, *Appl. Phys. Lett.* **68**, 3485 (1996).

¹⁸D. E. Aspnes and A. A. Studna, *Phys. Rev. B* **27**, 985 (1983).

¹⁹A. L. Beck, B. Yang, S. Wang, C. J. Collins, J. C. Campbell, A. Yulius, A. Chen, and J. M. Woodall, *IEEE J. Quantum Electron.* **40**, 1695 (2004).

²⁰S. M. Sze, *Physics of Semiconductor Devices* (Wiley, New York, 1981).